NOAA Technical Memorandum ERL ARL-64

DEPARTMENT OF COMMERCE
UNITED STATES OF AMERICA

A MESOSCALE TRANSPORT AND DIFFUSION MODEL

Roland R. Draxler

Air Resources Laboratory
Silver Spring, Maryland
June 1977

noaa NATIONAL OCEANIC AND ATMOSPHERIC ADMINISTRATION / Environmental Research Laboratories

NOAA Technical Memorandum ERL ARL-64

A MESOSCALE TRANSPORT AND DIFFUSION MODEL

Roland R. Draxler

Air Resources Laboratory
Silver Spring, Maryland
June 1977

UNITED STATES
DEPARTMENT OF COMMERCE
Juanita M. Kreps, Secretary

NATIONAL OCEANIC AND
ATMOSPHERIC ADMINISTRATION
Robert M. White, Administrator

Environmental Research
Laboratories
Wilmot N. Hess, Director

CONTENTS

LIST OF SYMBOLS

M = Mass, L = Length, T = Time, K = Degrees Kelvin Temp.

C	(ML^{-3})	-	Air concentration.
$\overline{C}_a$	(ML^{-3})	-	Average air concentration of material in a column subject to rainfall.
C_b	(L^{-1})	-	Normalized air concentration in the bottom box output from the finite difference diffusion model.
C_w	(ML^{-3})	-	Concentration of material in rainwater at the ground.
d	(L)	-	Distance from trajectory segment to wind station.
E		-	Dimensionless wet depletion scavenging ratio (4.2×10^5 by volume).
F	$(ML^{-2}T^{-1})$	-	Mass flux.
g	(LT^{-2})	-	Acceleration of gravity.
K_z	(L^2T^{-1})	-	Vertical mixing coefficient.
L	(L)	-	Depth of the layer subject to rainfall (4000 m).
P	(LT^{-1})	-	Precipitation rate.
Q	(M)	-	Amount of material in a pollutant puff.
R	(L)	-	Distance from the receptor to the center of the puff.
R_i		-	Richardson number.
r	(L)	-	Wind station averaging radius.
t	(T)	-	Diffusion time.
Δt	(T)	-	Time step within the finite difference model.
ΔT	(T)	-	Time interval for computation of trajectory segment displacements
u	(LT^{-1})	-	Wind speed.
$\vec{V}$	(LT^{-1})	-	Vector wind.
$\vec{V}_a$	(LT^{-1})	-	Vector adjusted surface wind.
v_d	(LT^{-1})	-	Dry deposition velocity.

χ		-	Dimensionless mixing ratio.
Z	(L)	-	Height.
ΔZ	(L)	-	Height differences.
ΔZ_i	(L)	-	Depth of a box in the finite difference model.
$\Delta Z_{\underline{i}}$	(L)	-	Distance between centers of adjacent boxes in the finite difference model.
α		-	Alignment weighting factor.
γ		-	Horizontal puff growth exponent.
δ	(L^{-2})	-	Distance weighting factor.
θ	(K)	-	Potential temperature.
$\overline{\theta}$	(K)	-	Mean potential temperature.
ρ	(ML^{-3})	-	Air density.
σ_h	(L)	-	Horizontal standard deviation of material in the puff.
ϕ		-	Angle between the wind direction and a line from the wind station to the trajectory segment starting point.
ξ	(L)	-	Linear vertical weighting factor.

A MESOSCALE TRANSPORT AND DIFFUSION MODEL

Roland R. Draxler
Air Resources Laboratories
Silver Spring, MD 20910

ABSTRACT

A mesoscale Lagrangian trajectory transport and diffusion model has been developed which takes into account stability changes along the trajectory. The required input data for trajectory computations are hourly surface meteorological observations and standard upper air observations. A one-dimensional finite difference model for vertical diffusion and deposition is used in the calculations with each trajectory. The vertical mixing coefficient is based upon the Pasquill stability at each trajectory segment. Dry deposition and washout are calculated if required. The transport layer, that layer containing 90% of the mass as calculated by the finite difference method, grows with time along the trajectory. Air concentrations are calculated for specified sampling periods at selected receptor locations.

1. INTRODUCTION

The Air Resources Laboratories (ARL) has developed a mesoscale trajectory transport and diffusion model which is designed to simulate the behavior of individual plumes and calculate short-term air concentrations. The transport is Lagrangian, in that the spatially averaged wind field near the trajectory segment is used to compute the displacement during each interval.

The trajectory computation method is similar to the one developed for continental-regional transport by Heffter and Taylor (1975), but utilizes a denser network of hourly surface observations. The input data come from a meteorological tape that combines hourly surface winds, temperature, dewpoint, pressure, total 6-hour precipitation, and calculated Pasquill stability classes. In addition, upper air observations of wind and temperature are included when available; usually every 12 hours.

Vertical diffusion is calculated concurrent with the transport. A one-dimensional (vertical) finite difference diffusion model is run with each trajectory. The vertical mixing coefficient is based upon the calculated Pasquill stability at each trajectory segment. Dry deposition and washout (determined from the observed precipitation) may be calculated along each trajectory. The vertical layer in the finite difference model containing 90% of the mass is considered the transport layer through which the upper air winds are averaged for the subsequent trajectory displacement calculation.

The upper air winds are linearly interpolated to the required time and spatially averaged by distance and alignment weighting factors in the layer determined from the vertical diffusion. The surface observations are made more frequently and are derived from a denser network than the upper air reports. The upper air soundings are used to determine adjustment factors to convert the surface winds to represent the desired layer winds. The adjusted surface winds are then considered to be the average transport winds for computing the trajectory displacement.

A pollutant puff is assumed to be released with each trajectory and average air concentrations are calculated for specified sampling periods at selected receptor locations. The vertical distribution of material in each puff is calculated by the finite difference model. The puff is then spread horizontally assuming a Gaussian distribution.

The chief advantages of this transport-diffusion method are that the height of the transport layer is allowed to increase as the emitted material spreads vertically, as determined by the stability conditions along each trajectory, and hourly surface weather data are incorporated.

2. MODEL INPUT REQUIREMENTS

2.1 Meteorological Input Data

An operational meteorological input data tape is produced prior to running the transport-diffusion model. This tape combines the data from two sources: U.S. Air Force Global Weather Center Surface Data extracted by the NOAA National Climatic Center (NCC, 1975) and upper level wind and temperature data extracted by ARL from the United States Air Force Environmental Technical Applications Center (USAF-ETAC, 1972) tapes (see Heffter and Taylor, 1975) available from NCC.

The NCC tape includes stations (and ships) located between 100°W and 60°W, 50°N and 20°N. About 600 surface observation stations report each hour in this area. The tapes of upper level data cover the continental United States and southern Canada; about 130 stations report every 12 hours. Although meteorological data are available worldwide from these sources, ARL's present interest is limited to the areas described.

The operational tape, where observations appear in time sequence, reduces tape manipulation and avoids repetitive operations. It can cover a reduced grid, for example the one shown in Figure 1. This area includes three states, and about 60 surface stations and 6 upper level stations (only 4 report regularly). One year of data can be written on a tape (9 track, 1600 bits per inch, binary format). Each three-digit number in Figure 1 indicates the percent reporting frequency for a particular station during the year 1975. A starred border indicates an upper air station. The frequencies are based on hourly observations for the surface stations and 12-hourly observations for the upper-air stations. The denser network and more frequent reports of the surface stations emphasize the utility of incorporating these data in any mesoscale model.

The surface observations on the NCC tape include 35 variables, many of them not needed for the present model structure. These have been reduced to

10: World Meteorological Organization block-station number, station longitude and latitude, station elevation above mean sea level (msl), wind direction, wind speed, station pressure, dry bulb temperature, dew point depression, and total 6-hour precipitation.

In addition to the above data, the estimated Pasquill stability category (A to G) is added to each surface observation. It is computed during the production of the operational tape and it follows the method given by Turner (1964), depending upon cloud cover, cloud ceiling, solar elevation angle, and wind speed. This method has been adopted by NCC in producing stability windroses at selected stations and is commonly referred to as the "STAR" (STability ARray) program. A complete description of the STAR method is given by Doty et al. (1976).

The upper air data, if available at a particular hour, follow the surface information on the tape. The first record gives the block station number, station longitude and latitude, station elevation, station height above average terrain (see Heffter and Taylor, 1975), and the number of levels of observations that follow. Each level contains the height of the observation above msl, the wind direction, wind speed, pressure, and temperature. No observations above 500 mb are included on the operational tape.

The upper level wind and temperature data on the ETAC tapes do not always appear at the same levels. To simplify data computations, temperatures and pressure were linearly interpolated to any wind levels where no corresponding temperature existed.

2.2 Transport and Diffusion Input Parameters

The computer code is divided into two sections; the input section and the main program. Input parameters that control model computations are utilized in two ways: parameters that are changed most frequently are read in on cards and those that change less frequently are assigned values within the input program. In the input section the dimensions of all arrays are computed. These dimensions are then substituted into the main program before execution begins.

Some of the frequently varied input parameters include:

a. location of the transport origin,
b. starting date,
c. the number of days of computations desired,
d. the time in days that each puff is followed,
e. the maximum height to which winds may be averaged, and
f. the boundaries of any output maps.

The values of some of the other trajectory parameters that may be changed include: the horizontal radius in which winds are to averaged (200 nmi for upper air stations and 75 nmi for surface stations), the number of trajectories started each day (24), the time interval for trajectory displacement computations (1 hour), and the height of the source (12 m).

Calculations of vertical diffusion in the finite difference model may include dry deposition (by specifying a deposition velocity) and washout (by specifying a precipitation rate or using the actual observed precipitation rate recomputed each 6 hours). The maximum value of vertical diffusivity that is currently specified for each Pasquill stability is given in Table 1. The origin of this table is discussed in more detail in section 3.1.

Table 1. Pasquill Stability and Vertical Diffusivity

Pasquill Stability Category	A	B	C	D	E	F	G
Vertical Diffusivity (m^2s^{-1})	50	30	15	7	3	1	0.3

Receptor locations must be specified for predictions of air concentration, and the frequency at which the pollutant puff is sampled (every 0.5 hours) at the receptor may vary. Horizontal puff growth may also be made dependent on Pasquill stability by specifying a growth rate for each stability category. At this time the growth rate is assumed to be the same for all stability categories.

3. VERTICAL TRANSPORT LAYER

A vertical diffusion finite difference model is run with each trajectory (pollutant puff). The extent of the vertical distribution of material determines through which layer the winds are to be averaged for computation of the trajectory transport. The rate of vertical mixing depends upon the magnitude of the mixing coefficients, K_z, specified at each box boundary.

3.1 Vertical Mixing Coefficients

The vertical mixing coefficient profile that controls the vertical diffusion for a trajectory segment is determined from the Pasquill stability and Richardson number profile at the observation points nearest that trajectory segment starting point.

First a value of K_z at 150 m is selected on the basis of the Pasquill stability (Table 1). The K_z below 150 m is given by

$$K_z\ (<150\ m) = K_z\ (at\ 150\ m) \bullet Z/150, \quad (1)$$

and K_z is constant above 150 m. The values in Table 1 have been determined by dividing the likely range of values of K_z into seven arbitrary intervals. This range of K_z has been determined from the results of studies by Shaffer (1973) and Guedalia et al. (1974). A summary of data from Shaffer (1973) is shown in Figure 2. He determined K_z from Radon flux measurements on a tower. Diurnal variations of K_z were averaged for several months.

Second, the K_z profile for the appropriate stability category is then reduced to a low value, 0.1 m^2s^{-1}, in those layers where the Richardson number, given by

$$R_i = \frac{g(Z_2 - Z_1)}{\bar{\theta}} \frac{(\theta_2 - \theta_1)}{(u_2 - u_1)^2} \quad (2)$$

exceeds a preselected value, and where subscript 2 is the upper observational level and subscript 1 is the lower level. These low values of K_Z simulate the stable layers where a limited exchange of mass occurs.

The upper-level soundings are usually taken every 12 hours. Therefore the soundings are linearly interpolated to the same interval that trajectories are started. The results probably do not adequately reflect the diurnal changes in the planetary boundary layer. One of the planned uses of the transport-diffusion model is the simulation of special case studies, and for these it is likely that more frequent meteorological sounding data will be available.

3.2 Vertical Diffusion Finite Difference Model

The finite difference model is a one-dimensional (vertical) box model in which the rate of diffusion is determined by specifying K_Z at the box interfaces. K_Z may change with height and time as described in the previous section. One advantage of the finite difference method is that it permits deposition to be treated in a more realistic fashion. Material is removed from the lowest box rather than the loss being distributed instantaneously throughout the column, as is done in the widely used "source depletion" method of Chamberlain (see Van der Hoven, 1968).

The finite difference method follows the one developed by Machta (1966) for large scale diffusion. We consider a column of unit horizontal area divided into boxes of various heights. A particular box is denoted by i, and values appropriate to the upper and lower boundaries of the box are denoted by $\bar{i}$ and $\underline{i}$ respectively.

The net flux of material, F_i, into the i-th box is given by

$$F_i = \left[K_Z \, \rho \, \partial X / \partial Z \right]_{\bar{i}} - \left[K_Z \, \rho \, \partial X / \partial Z \right]_{\underline{i}} . \quad (3)$$

The change with respect to time of the mixing ratio of the i-th box of vertical extent ΔZ_i is expressed as

$$\partial X / \partial t = F_i \, \rho_i^{-1} \, \Delta Z_i^{-1} . \quad (4)$$

Equations 3 and 4 are solved numerically through finite difference approximations forward in time and centered in ΔZ. A more complete description of this diffusion model, including tests of the effects of diurnal stability variations with various dry deposition velocities, has been reported by Draxler and Elliott (1977).

To maintain computational stability and to minimize computer time, the time step is reevaluated for the K_z profile that applies to the diffusion during each trajectory segment. The time step, given by

$$\Delta t = 0.25 \, \Delta Z_{\underline{i}}^2 \, K_{z_{\underline{i}}}^{-1} \tag{5}$$

is evaluated at each box interface and the smallest value of Δt for the K_z profile is used for the computation.

At present, there are 20 boxes, in 4 groups of 5 boxes, the lowest are 25 m each, then 50 m, 100 m and 250 m to the top of the model for a total model depth of 2125 m. More boxes may be added in order to deal with a deeper mixed layer. No diffusion is permitted through the top of the model, but dry deposition from the bottom box can occur, as well as wet deposition from all boxes. A unit source is injected into a preselected box for each trajectory.

For dry deposition, the deposition velocity (v_d) multiplied by the concentration in the lowest box (#1) gives the mass deposited per unit time. The mixing ratio in the lowest box after dry deposition is given by

$$X_{(1,t + \Delta t)} = X_{(1,t)} \left[1 - v_d \, \Delta t / \Delta Z_1 \right], \tag{6}$$

where $X_{(1,t)}$ is the mixing ratio in the lowest box before deposition.

Although it is possible to modify the deposition velocity with each trajectory segment, at present a constant deposition velocity is used for all trajectories.

According to the method of Heffter and Ferber (1975), wet deposition is calculated using an average scavenging ratio (4.2×10^5) derived from Engelmann (1970). The scavenging ratio is defined by

$$E = C_W / \overline{C}_a, \tag{7}$$

where $\overline{C}_a$ is the average concentration of material in the air and C_w is the concentration of material in the rainwater at the ground.

The mixing ratio of material in the boxes after wet deposition is given by

$$X_{(i,t + \Delta t)} = X_{(i,t)} \left[1 - \frac{E \, P \, \Delta t}{L} \right], \tag{8}$$

where $X_{(i,t)}$ is the mixing ratio before wet deposition, P is the precipitation rate, and (i) includes all the boxes within the rain layer, L. The rain layer need not have the same vertical extent as the model. The precipitation rate is determined from the meteorological input data. The 6-hour total precipitation observations ending at 00, 06, 12, and 18 GMT are reported. The precipitation rate used for wet deposition computations is obtained from the nearest reporting station at the next observation time. The precipitation rate is assumed to be uniform during the observation period.

Figures 3a, 3b, 3c, and 3d show a time sequence of a precipitation field for 1 day. Values shown are the 6-hour totals in millimeters. These figures suggest that the 6-hour frequency provides sufficient resolution for the mesoscale network.

The finite difference model is run for the duration of the trajectory segment, usually one hour. After the diffusion computation is completed for a segment, air concentrations in the lowest box (ground level) are saved for later use. Also the vertical layer which contains 90% of the mass is computed. This layer represents the transport layer in which the winds are to be averaged to compute the next trajectory endpoint. In this way, the computations allow pollutant puffs to respond to a variety of stability conditions during transport. For instance, vertical growth would be inhibited at night and enhanced during the day. After most of the material is distributed aloft, subsequent stability changes would not affect the transport layer, unless dry deposition alters the vertical air concentration profile.

4. TRAJECTORY SEGMENT DISPLACEMENT

Each trajectory segment endpoint is computed assuming wind persistence for the duration of the segment. The winds are vertically averaged within the transport layer for stations within a prescribed radius of the segment starting points.

The upper level stations report only every 12 hours; therefore the network of surface station winds is incorporated for the trajectory displacement calculation in order to improve the simulation of mesoscale transport.

4.1 Vertical and Horizontal Averaging of Winds

The averaging method used is identical to that described by Heffter and Taylor (1975). The average wind in the layer is computed from the reported winds at levels linearly weighted by the thickness between the mid-levels. The vertically averaged layer wind for station (j) is given by

$$\vec{V}_j = \frac{\Sigma \xi_i \vec{V}_i}{\Sigma \xi_i} , \qquad (9)$$

where

$$\xi_i = \left[\frac{Z_{i+1} + Z_i}{2}\right] - \left[\frac{Z_i + Z_{i-1}}{2}\right] , \qquad (10)$$

and (i) specifies the observation level. In Equation 10, the first term cannot exceed the top of the transport layer, and the last term cannot be less than the base of the transport layer.

The averaged layer wind from stations within radius r of the segment starting point are weighted and averaged according to an alignment and distance factor. The final average wind for all stations within radius r is given by

$$\vec{V} = \frac{\Sigma\, \delta_j\, \alpha_j\, \vec{V}_j}{\Sigma\, \delta_j\, \alpha_j}, \qquad (11)$$

where $\vec{V}_j$ is the averaged layer wind from Equation 9 for that station. The alignment weight

$$\alpha_j = 1 - 0.5 \left| \sin \phi_j \right| \qquad (12)$$

and the distance weight

$$\delta_j = d_j^{-2}, \qquad (13)$$

where d_j is the distance from the observed wind to the midpoint of the trajectory segment ($\frac{1}{2}\, \Delta T\, \vec{V}_j$) that would be produced from the wind at that station, and ϕ is the angle between the wind direction and the line from the observation point to the trajectory segment starting point. Alignment weighting is introduced in order to give the observations upwind and downwind from the segment starting point the greatest weight.

4.2 Use of the Surface Wind Network

The network of surface weather stations are utilized in computing trajectories. The displacement of the endpoint is determined from an adjusted surface wind times the time interval between segments. A layer wind is developed at the surface station on the basis of the relationship between the layer and surface wind at the upper air station. The steps are:

a. A spatially averaged layer wind from the upper air stations is computed (Eqs. 9 and 11).

b. A spatially averaged surface wind ($\vec{V}_j = \vec{V}_i$ for i=1) from the upper air stations is computed (Eq. 11).

c. The directional change and ratio of wind speeds between the averaged surface (b) and layer (a) wind are determined.

d. A spatially averaged surface wind from the surface stations is computed (Eq. 11).

e. The average wind from (d) is adjusted to represent a layer wind by the directional change and speed ratio determined in (c).

The final wind computed in (e) is used for the trajectory segment displacement.

The direction and speed ratios are recorded for each segment and printed in tabular form. Generally, as the puff grows vertically, the directional change and speed ratio of layer wind to surface wind increases.

One problem with the surface wind adjustment method is the infrequent upper level observations. These observations have been interpolated to hourly values so that direct comparison with hourly observed surface-data could be made. The travel time over the mesoscale region is about the same order as the frequency of the upper level observations, so these data are unsatisfactory as the only meteorological input. It is believed that the uncertainties in the surface wind adjustment are outweighed by the benefits derived from more frequent observations and denser coverage, especially when all the averaging procedures are considered.

5. RECEPTOR-ORIENTED PUFF DIFFUSION MODEL

A puff of pollutant material is assumed to be released with each trajectory. When trajectories are started each hour, for example, the material in the puff is set equal to the mass of material emitted from the source during one hour.

The vertical diffusion of a puff (including any dry and wet deposition) is computed by the finite difference method during the transport calculations. The surface air concentration is calculated at each trajectory segment endpoint for a column of unit horizontal area.

The horizontal distribution of material (Heffter and Ferber, 1975) at a trajectory segment endpoint when expanded in a Taylor series is given by

$$\sigma_h\,(t+\Delta T) = \sigma_h\,(t) + \Delta T\,\frac{d\sigma_h}{dt} \qquad (14)$$

where

$$\frac{d\sigma_h}{dt} = 0.5\,\gamma\,t^{(\gamma-1)}, \qquad (15)$$

and t is in seconds and σ_h in meters. The horizontal growth exponent, γ, is dependent upon the Pasquill stability at each trajectory segment. Faster growth rates are indicated by larger values of γ. When $\gamma = 1.0$, Equation 14 reduces to that given by Heffter and Ferber (1975). At this time the variation of γ with stability is uncertain, and $\gamma = 1.0$ is used for all cases.

Several receptor locations may be selected. As the center of the puff passes within $4\sigma_h$ of a receptor, the surface air concentration at the receptor is given by

$$C = Q\,C_b\,\frac{1}{2\pi\,\sigma_h^2}\,\exp\frac{-R^2}{2\sigma_h^2}, \qquad (16)$$

where C_b is the normalized air concentration from the finite difference model (the mixing ratio in the lowest box times the air density divided by the initial unit source).

The concentration contributions from each puff that passes the receptor during a selected sampling period are summed. The final output lists the average air concentration for each sampling period and the contribution from each puff that passed within $4\sigma_h$ during the sampling period.

The interval at which puff concentrations are recorded at a receptor may be varied. If puffs are sampled too infrequently, some may pass the receptor without contributing to the computed air concentration. The proper puff sampling interval depends upon the puff size and the transport speed. If one assumes that puffs should be sampled at least every one σ_h, $\gamma = 1.0$ (Eqs. 14 and 15), and that the mean transport speed is 5 ms^{-1}, then the sampling interval is as given in Table 2 for several downwind receptor distances.

Table 2. Suggested Puff Sampling Interval

Receptor Distance (km)	10	20	40	80	160
Sampling Interval (min)	3	7	14	27	54

6. DESCRIPTION OF THE COMPUTER CODE OUTPUT

Each section that follows describes the computer output from the model in the order the output is printed. Examples are shown for each section. On some computer output tables the right side has been deleted to avoid reducing the size of the table.

6.1 Title Page

The first output page shown in Figure 4 lists some of the program variables. The first group consists of the input cards:

a. An identification and latitude and longitude of the trajectory starting position.

b. The starting date (day, month, year).

c. The number of days of computations.

d. The duration in days that each trajectory is followed.

e. The number of days of meteorological input data.

f. The lower and upper limits of the transport layer in meters.

g. The boundaries (latitude and longitude) of the mercator projection for any output maps.

The second group is a collection of parameters that influence the trajectory computation. These may also be changed, but within the computer code. Numbers in parentheses are values currently in use.

a. The number of trajectories started each day (24 or one each hour).

b. The trajectory segment duration, which is the interval at which the winds are sampled and averaged to compute each segment endpoint (1 hour).

c. The number of input winds per day (24 with the input tape described in this paper).

d. The number of interpolated winds per day. (24—only the less frequent upper level winds are interpolated.)

e. The upper level scan radius is the radius within which the winds at the upper level stations are averaged (200 nautical miles).

f. The surface scan radius is the radius within which the winds at the surface stations are averaged (75 nautical miles).

The third group consists of diffusion-deposition parameters.

a. The box number in the finite difference model (bottom box = 1) in which the initial source material is injected.

b. The dry deposition velocity in cm s^{-1}.

c. The precipitation rate in m s^{-1}. It is non-zero when a constant precipitation is assumed for all trajectories and zero when the actual observed precipitation is used.

d. The number of times a puff is sampled during a trajectory segment (ΔT/Table 2 sampling interval).

6.2 Meteorological Input Data

An example of the numbers of meteorological stations tabulated on the input tape for each observation is reproduced in Figure 5. On the grid shown in Figure 1 about 60 surface stations report hourly and about 4 upper level wind stations report at 12-h intervals. Temperature soundings are listed separately because they are not always reported with the wind sounding.

6.3 Trajectory Segment Computation Table

An example of the number of surface wind stations within radius r used to compute the average wind and the Pasquill stability for each trajectory segment is shown in Figure 6. The trajectory starting time is in the left column. The two rows to the right of the starting time tabulate the information for each segment of that trajectory, by segment number (one each hour). For the trajectory starting on December 1 at 00Z, segment number 12 would represent that trajectory after 12 hours. Seven surface stations were within the averaging radius and the Pasquill stability category was "D". A blank space between the number of stations and stability category indicates that the winds were averaged as described in this note. A symbol in this space indicates that not all the data were available. These symbols are identified in Table 3.

Table 3. Trajectory Wind Code

Code	Meaning	Program Action
U	Average wind at upper level station is calm.	Use interpolated layer wind at upper level stations. The number of stations within the radius listed would be upper air stations.
V	No surface stations within radius.	(as above)
W	Average surface wind is calm.	(as above)
X	No upper level stations within radius.	Use unadjusted wind at surface stations.
•	No surface stations in radius and no upper level stations in radius.	End trajectory.

Segment 36, just below segment 12, for the same trajectory (1 Dec. 00Z) shows "2V" which means that 2 upper level stations were used for transport calculations because no surface stations were within the radius. A blank for the stability in the third print position means that it was not possible to compute the stability at that time and a "D" was assumed. At segment 38, the trajectory was ended for lack of data over the Atlantic Ocean.

6.4 Bottom and Top of the Transport Layer

Figure 7 gives the computed bottom and top of the transport layer for each trajectory segment. Two digits for bottom and two for top represent height in hundredths of meters. When no value is given for the bottom, 0 meters is assumed and the space is left blank. A "120" would mean the layer was from 100 to 2000 m. A 9999 is printed after a trajectory has ended. Comparison with stabilities from Figure 6 shows that the transport layer grows more quickly during unstable Pasquill stabilities than during more stable conditions.

6.5 Lowest and Highest Stable Layer

Figure 8 gives the lowest and highest level in hundredths of meters where the Richardson number exceeded the preselected value. The heights are read the same way as in Figure 7. These two levels, and possibly others in between, are where the value of K_Z has been reduced to simulate restricted mixing. The finite difference model is set for a maximum of 2125 m at present; however, stable layers may be indicated to the maximum height of the observed data (about 5000 m).

6.6 Wind Direction Change and Wind Speed Shear

The adjustment applied to the spatially averaged surface wind at each segment is given in Figure 9. The first two digits represent the value in degrees added to the average wind direction. A positive number indicates veering with height. A value of 98 indicates an addition of 98 degrees or greater. A value of 99 indicates the trajectory has been terminated. The last two digits represent the value (times 10) by which the surface wind speed was multiplied; for instance, 19 indicates that the average surface wind was multiplied by 1.9. A value of 98 is for 9.8 and greater, and 99 indicates the trajectory has been terminated.

6.7 Trajectory Segment Endpoints

Figure 10 lists the latitude and longitude of each trajectory segment endpoint after a specified number of hours (rather than by segment number). This print interval may be varied. The positions are given in hundredths of a degree. The position of a terminated trajectory is given by 9999.

6.8 Mercator Trajectory Plot

Trajectory segment endpoint positions are plotted on a Mercator projection in Figure 11. The plotted symbols that represent the different trajectory starting times are shown in the upper portion of Figure 12. Four trajectories are plotted on a map. For instance, the trajectory that was started at 12Z is represented by the letter "M". The 2-hour position (14Z) along the "M" trajectory is represented by the symbol "1", the 4-hour position (16Z) by the symbol "2". This code is given in the lower portion of Figure 12. The geographic boundaries are produced in another program and are not a normal part of the output from the line printer.

6.9 Receptor Diffusion Model

In Figure 13 a sample page from the diffusion model output is shown. The top line identifies the method of vertical diffusion, in this case the finite difference (box) model, the dry deposition velocity, and the precipitation rate. The second line indicates that actual precipitation was used. In this case the precipitation rate on the top line is the average value that occurred for all trajectory segments normalized to one year. If an average value is assumed for all trajectories, then that value is shown. The third line gives the receptor identification and location. The following groups are the sampling windows, in this case one each hour. The digits under the column headed DATE identify the time the sampling window directly to the right begins. The first group of three windows (100) starts at 00Z on the 1st. The second group of three windows following below (103) starts at 03Z on the 1st. The third window of each group has been deleted from the figure.

In any one window, for example 12Z on the 1st (112), 55.566 represents the concentration including a specified background; 42.566 is the concentration above background. The numbers in the next column give the concentration from each puff contributing to that window (12Z to 13Z), with the time that the puff left the source in parentheses. The puff that left on the 1st, 0800Z contributed 0.12 E+01 (1.2). Concentration units depend upon the source term.

7. CONCLUDING REMARKS

The model described here is only a first step. Further refinement of the wind averaging and transport methods, and horizontal and vertical diffusion schemes will be guided by the results of a model verification study. The routine emissions of Kr-85 from the Savannah River nuclear fuel reprocessing plant have been sampled at 13 locations within 140 km of the plant. Weekly samples have been collected at these locations for over 2 years and twice-daily samples were obtained during some periods. The measured Kr-85 concentrations will be compared with model predictions.

8. ACKNOWLEDGMENT

Gilbert J. Ferber and others at ARL had many helpful comments during all stages of this work. Albion D. Taylor provided valuable assistance during the development of the computer code.

9. REFERENCES

Doty, S.R., B.L. Wallace, and G.C. Holzworth, 1976: A Climatological Analysis of Pasquill Stability Categories Based on "STAR" Summaries. NOAA EDS NCC, Asheville, NC 28801, 51 p.

Draxler, R.R. and W.P. Elliott, 1977: Long Range Travel of Airborne Material Subject to Dry Deposition, Atmos. Environ., 11(1): 35-40.

Engelmann, R.J., 1970: Scavenging Prediction Using Ratios of Concentrations in Air and Precipitation, Proc. Symp. on Precipitation Scavenging, AEC Symp. Ser. 22, pp. 475-485.

Guedalia, D., C. Allet, and J. and Fontan, 1974: Vertical Exchange Measurements in the Lower Troposphere Using ThB (Pb-212) and Radon (Rn-222), J. Appl. Meteorol., 13, pp. 27-39.

Heffter, J. L. and G.J. Ferber, 1975: Diffusion-Deposition Models, Part II, A Regional-Continental Scale Transport, Diffusion and Deposition Model, NOAA Tech. Memo, ERL ARL-50, 28 p.

Heffter, J.L. and A.D. Taylor, 1975: Trajectory Model, Part I. A Regional-Continental Scale Transport, Diffusion and Deposition Model, NOAA Tech. Memo. ERL ARL-50, 28 pp.

Machta, L., 1966: Some Aspects of Simulating Large Scale Atmospheric Mixing, Tellus, 18: 355-362.

National Climatic Center, 1975: U.S.A.F. Global Weather Central Surface Data, NOAA EDS NCC, Asheville, NC 28801, NCC Library TD9687.

Shaffer, W.A., 1973: Atmospheric Diffusion of Radon in a Time-Height Regime, Ph.D. Thesis, Drexel Univ., June, 109 p., University Microfilms, Ann Arbor, Michigan.

Turner, D.B., 1964: A Diffusion Model for an Urban Area, J. Appl. Meteorol. 3(1): 83-91.

USAF-ETAC, 1972: DATSAV-SYNFILE Upper-Air Meteorological Data, Washington, Navy Yard Annex, Washington, DC.

Van der Hoven, I., 1968: Deposition of Particles and Gases, in Meteorology and Atomic Energy, edited by D.H. Slade, pp. 202-208, USAEC Division of Technical Information, Oak Ridge, TN, TID-24190.

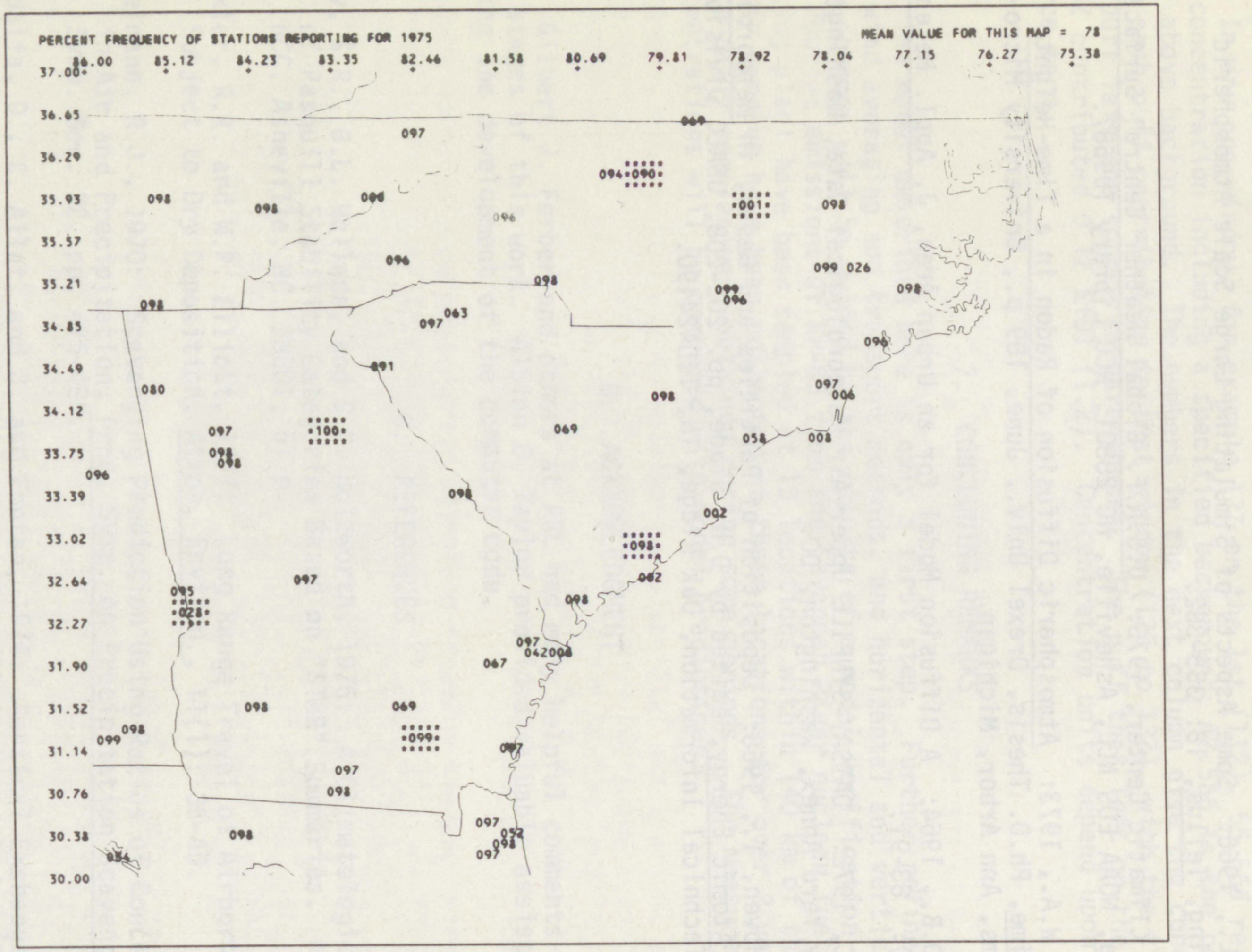

Figure 1. The percent frequency of stations reporting on the reduced grid of the operational meteorological input tape. A starred border indicates an upper-air station and the rest are surface stations.

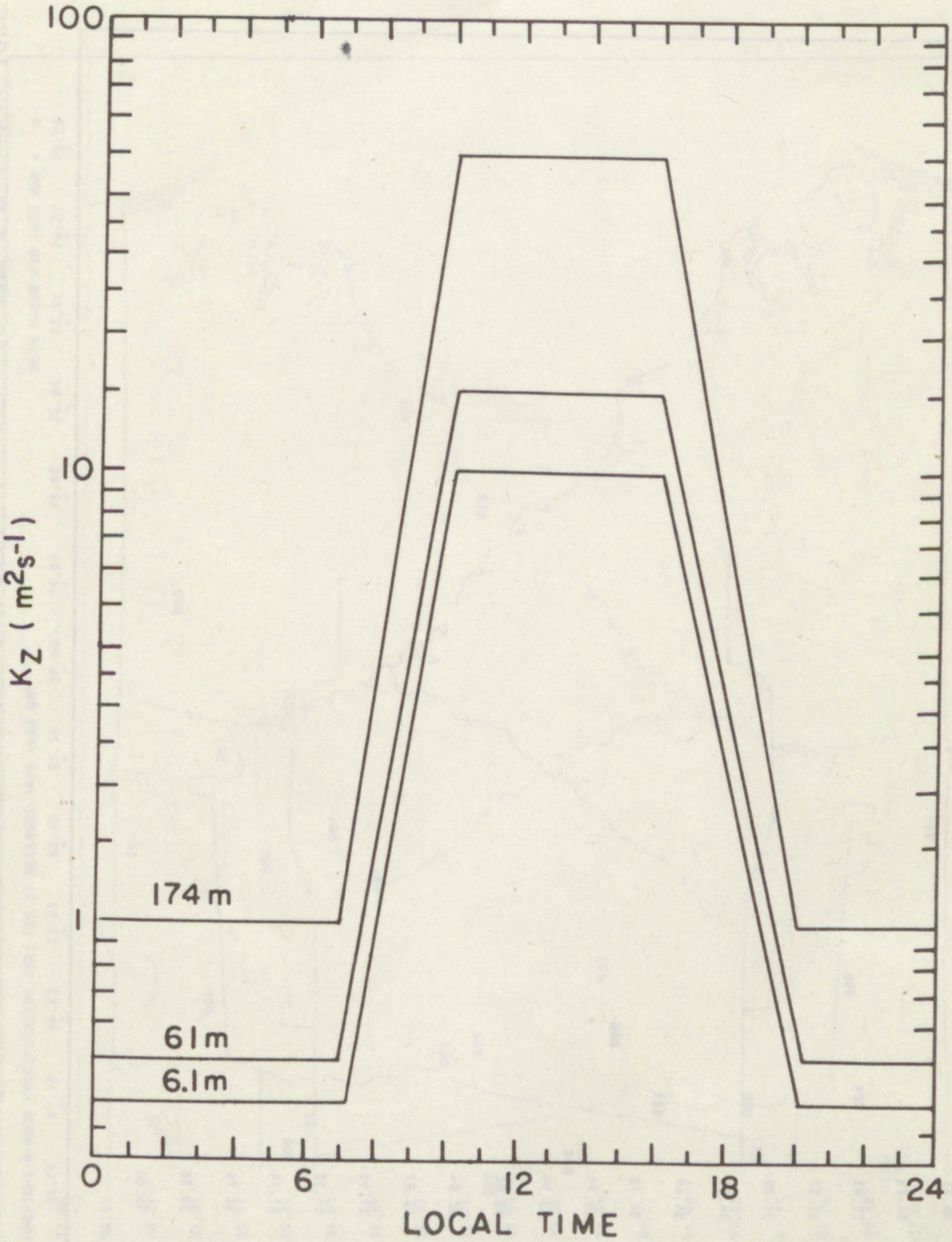

Figure 2. A composite set of K_z profiles adapted from Shaffer (1973).

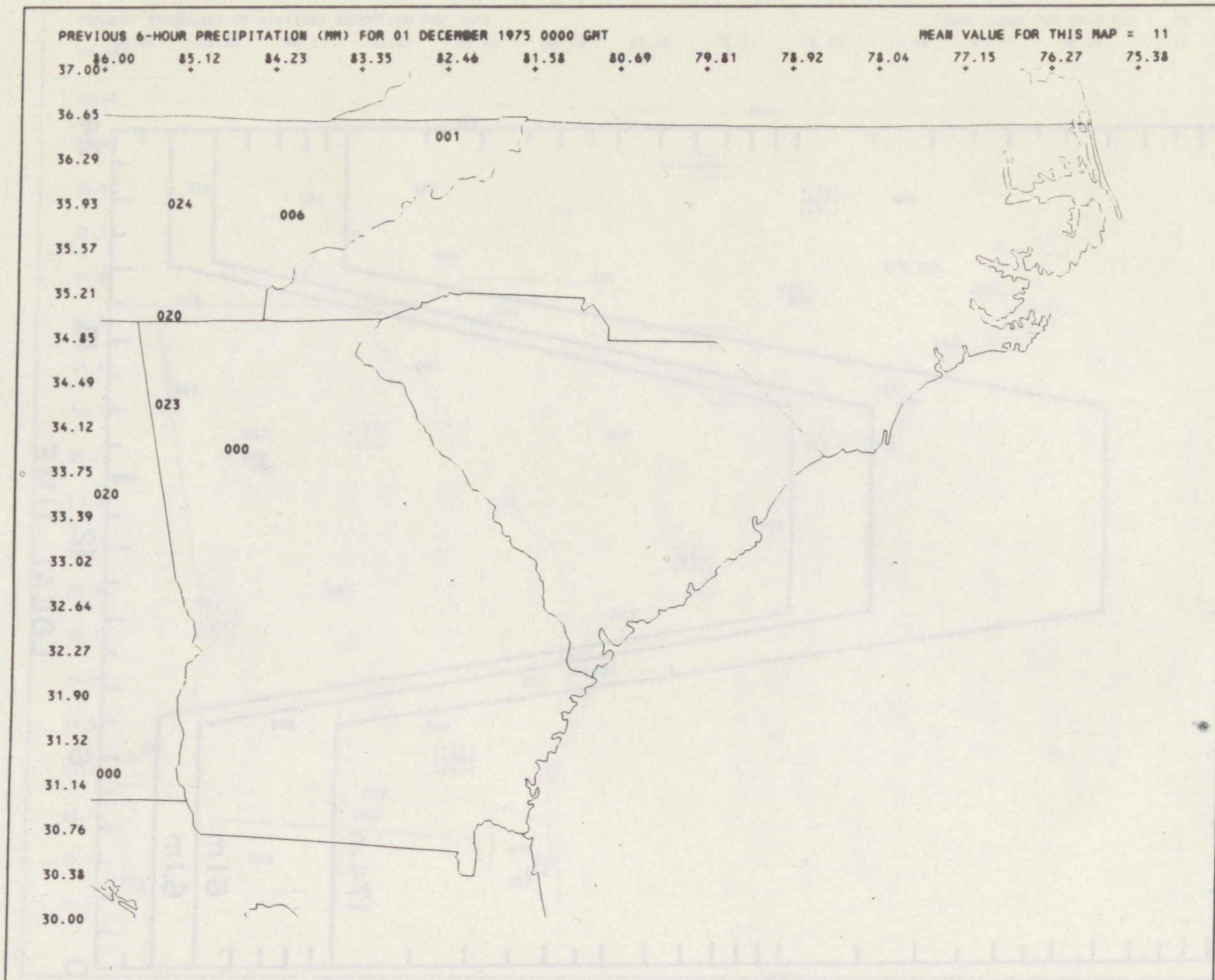

Figure 3a. The previous 6 h precipitation in millimeters for 00 GMT 1 December 1975.

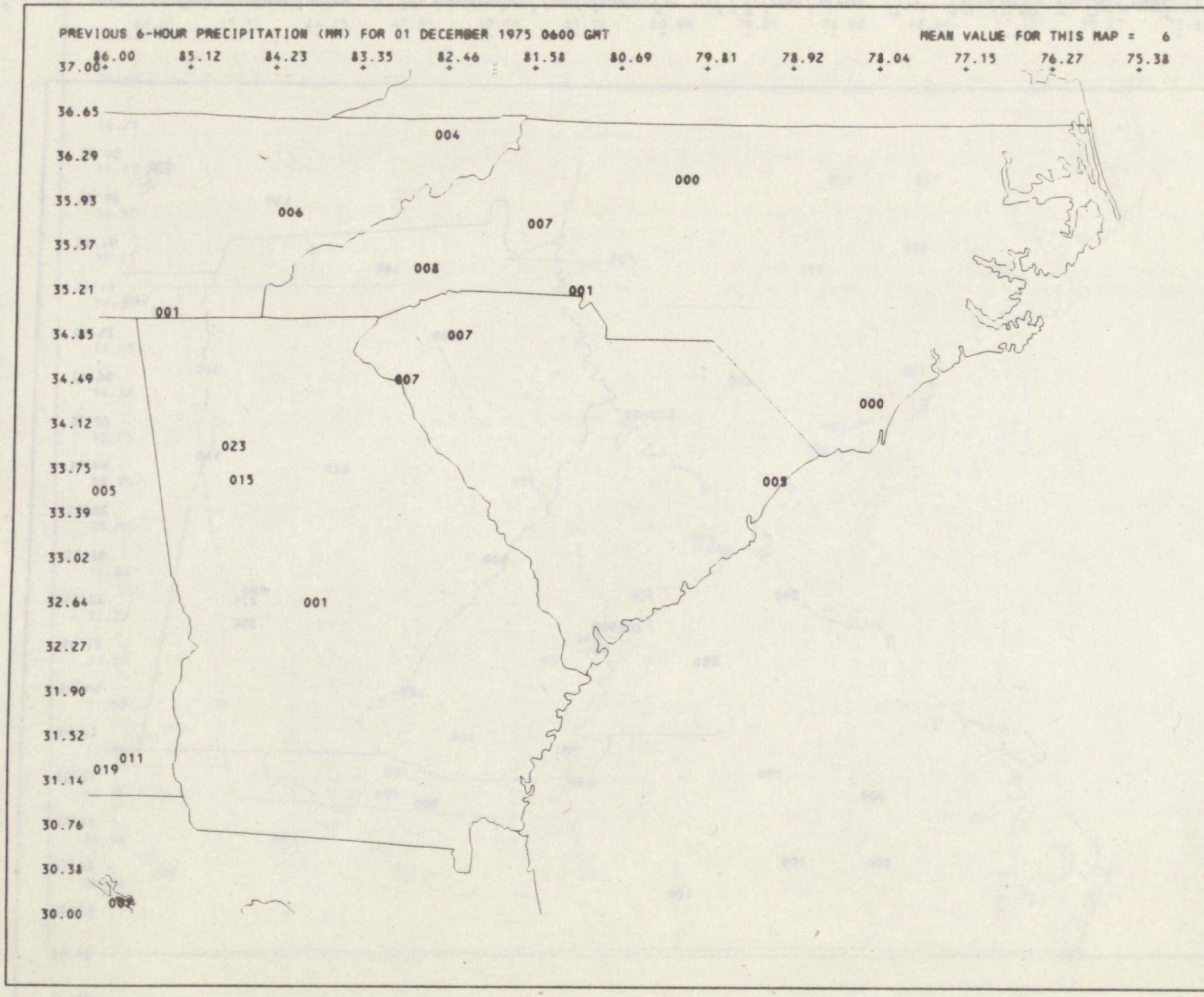

Figure 3b. The previous 6 h precipitation in millimeters for 06 GMT 1 December 1975.

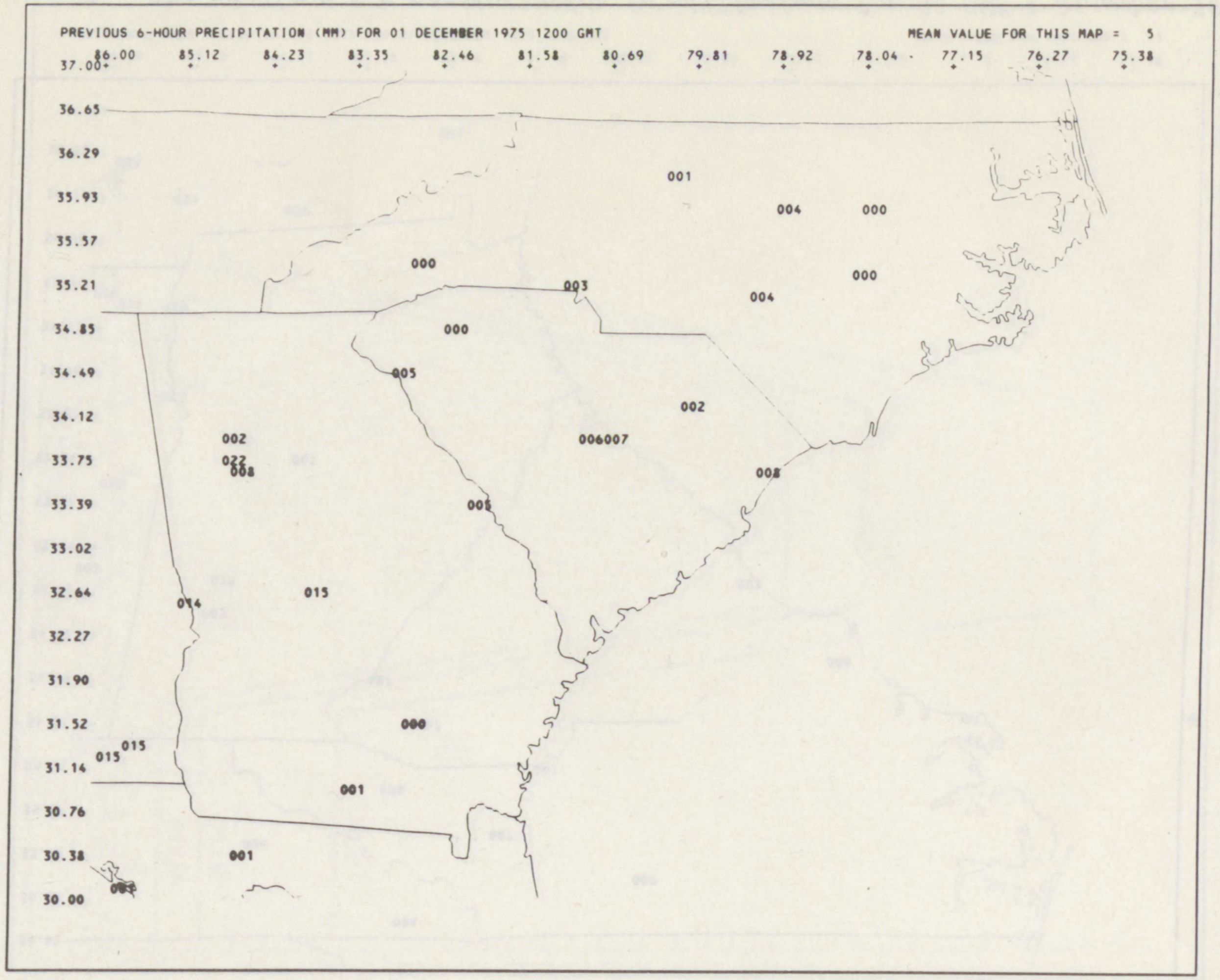

Figure 3c. The previous 6 h precipitation in millimeters for 12 GMT 1 December 1975.

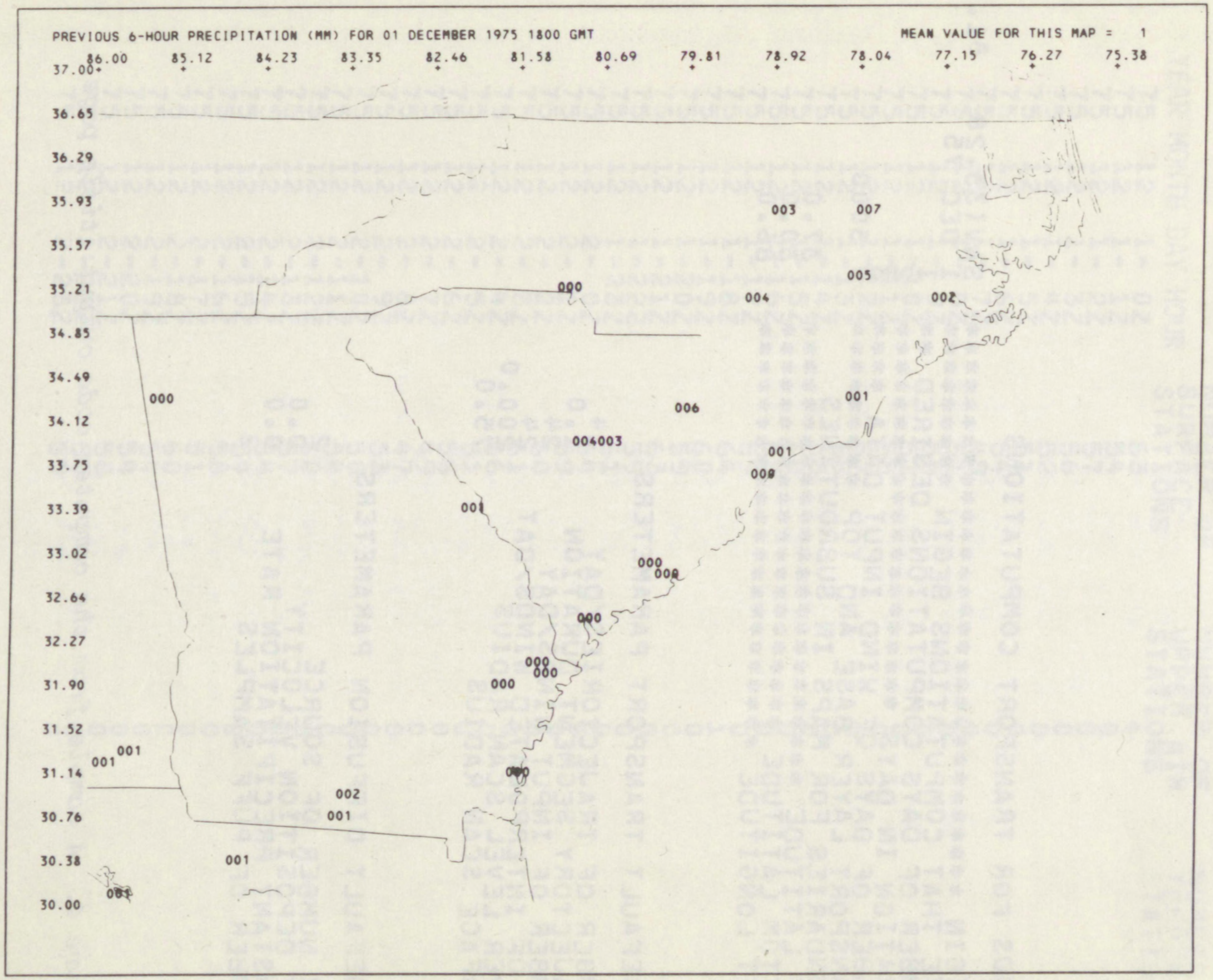

Figure 3d. The previous 6 h precipitation in millimeters for 18 GMT on 1 December 1975.

```
INPUT CARDS FOR TRANSPORT COMPUTATIONS

     ORIGIN ***********************************  SAV(33.28   81.66)
     DATE THAT COMPUTATIONS BEGIN **********     1 DEC 75
     NUMBER OF DAYS COMPUTATIONS DESIRED **      1
     DURATION IN DAYS ***********************    2
     NUMBER OF DAYS OF WIND INPUT DATA ****      3
     TRANSPORT LAYER BASE AND TOP **********     0 5000
     BOUNDARIES FOR MAPS IN SUBROUTINES
     TOP LATITUDE ****************************    37.0
     BOTTOM LATITUDE *************************    30.0
     LEFT LONGITUDE **************************    86.0


PROGRAM DEFAULT TRANSPORT PARAMETERS

     NUMBER OF TRAJECTORIES/DAY       24
     TRAJECTORY SEGMENT DURATION      1.0
     NUMBER OF INPUT WINDS/DAY        24
     NO OF INTERPOLATED WINDS/DAY     24
     UPPER LEVEL SCAN RADIUS          200.0
     SURFACE SCAN RADIUS              75.0


PROGRAM DEFAULT DIFFUSION PARAMETERS

     BOX NUMBER OF SOURCE             2
     DRY DEPOSITION VELOCITY          0.0
     CONSTANT PRECIPITATION RATE      0.0
     NUMBER OF PUFF SAMPLES           2
```

Figure 4. A sample from the computer code output: title page.

YEAR	MONTH	DAY HOUR	NUMBER OF SURFACE STATIONS	NUMBER OF UPPER AIR STATIONS	NUMBER OF TEMPERATURE STATIONS
75	12	1- 0Z	63	4	4
75	12	1- 1Z	54	0	0
75	12	1- 2Z	57	0	0
75	12	1- 3Z	56	0	0
75	12	1- 4Z	52	0	0
75	12	1- 5Z	51	0	0
75	12	1- 6Z	54	0	0
75	12	1- 7Z	49	0	0
75	12	1- 8Z	51	0	0
75	12	1- 9Z	55	0	0
75	12	1-10Z	51	0	0
75	12	1-11Z	55	0	0
75	12	1-12Z	67	5	5
75	12	1-13Z	59	0	0
75	12	1-14Z	58	0	0
75	12	1-15Z	60	0	0
75	12	1-16Z	60	0	0
75	12	1-17Z	59	0	0
75	12	1-18Z	64	1	0
75	12	1-19Z	60	0	0
75	12	1-20Z	59	0	0
75	12	1-21Z	63	0	0
75	12	1-22Z	59	0	0
75	12	1-23Z	61	0	0
75	12	2- 0Z	64	4	4
75	12	2- 1Z	59	0	0
75	12	2- 2Z	60	0	0
75	12	2- 3Z	61	0	0
75	12	2- 4Z	56	0	0
75	12	2- 5Z	51	0	0
75	12	2- 6Z	56	0	0
75	12	2- 7Z	49	0	0
75	12	2- 8Z	47	0	0
75	12	2- 9Z	53	0	0
75	12	2-10Z	50	0	0
75	12	2-11Z	54	0	0
75	12	2-12Z	62	5	3
75	12	2-13Z	57	0	0
75	12	2-14Z	54	0	0
75	12	2-15Z	54	0	0
75	12	2-16Z	58	0	0
75	12	2-17Z	51	0	0
75	12	2-18Z	60	0	0
75	12	2-19Z	54	0	0
75	12	2-20Z	54	0	0
75	12	2-21Z	58	0	0
75	12	2-22Z	50	0	0
75	12	2-23Z	59	0	0

Figure 5. A sample from the computer code output: meteorological input.

START DATE-TIME DEC 75	TRAJECTORY SEGMENT 1 25	2 26	3 27	4 28	5 29	6 30	7 31	8 32	9 33	10 34	11 35	12 36	13 37	14 38	15 39
1- 0Z	6 F 9 D	5 E 7 E	5 E 4 D	3 D 3 E	4 E 3 F	4 D 3 E	4 D 4 F	5 D 2 F	5 D 2V	5 D 2V	5 D 2V	7 D 2V	8 D 1	8 D 0.	7 D 0
1- 1Z	6 E 7 E	6 E 4 D	4 D 3 E	3 E 3 F	4 D 3 E	4 D 4 F	5 D 2 F	5 D 2V	5 D 2V	5 D 2V	7 D 2V	8 D 2V	8 D 0.	7 D 0	8 D 0
1- 2Z	6 E 4 D	5 D 3 E	3 E 3 F	3 D 3 E	4 D 4 F	5 D 2 F	5 D 2V	5 D 2V	5 D 2V	7 D 2V	8 D 1	8 D 0.	7 D 0	8 D 0	8 D 0
1- 3Z	6 D 3 E	5 E 5 F	3 D 3 E	4 D 4 F	6 D 3 F	6 D 2 D	6 D 2V	6 D 2V	6 D 2V	8 D 1	8 D 0.	7 D 0	8 D 0	7 D 0	6 D 0
1- 4Z	6 E 5 F	4 D 4 E	3 D 4 F	4 D 3 F	6 D 3 D	6 D 2V	6 D 2V	6 D 2V	8 D 1	8 D 0.	7 D 0	8 D 0	7 D 0	5 D 0	5 D 0
1- 5Z	5 D 4 E	4 D 5 F	3 D 3 F	4 D 3 D	6 D 2 D	6 D 2V	6 D 2V	8 D 1	8 D 2V	7 D 2V	8 D 0.	7 D 0	5 D 0	5 D 0	7 D 0
1- 6Z	5 D 5 F	4 D 4 F	4 D 3 D	4 D 3 D	5 D 2V	6 D 2V	7 D 1	8 D 2V	7 D 2V	8 D 0.	6 D 0	5 D 0	5 D 0	6 D 0	7 D 0
1- 7Z	5 D 3 F	3 D 3 D	4 D 2 D	4 D 2V	6 D 2V	7 D 1	6 D 2V	7 D 2V	7 D 2V	6 D 0.	5 D 0	5 D 0	7 D 0	7 D 0	9 D 0
1- 8Z	5 D 3 D	4 D 2VD	3 D 2V	3 D 2V	5 D 1	6 D 2V	6 D 2V	5 D 0.	5 D 0	5 D 0	5 D 0	8 D 0	8 D 0	9 D 0	9 D 0
1- 9Z	5 D 2V	4 D 2V	4 D 2V	4 D 1	4 D 2V	4 D 0.	6 D 0	5 D 0	6 D 0	6 D 0	7 D 0	8 D 0	10 D 0	9 D 0	8 D 0
1-10Z	5 D 2V	4 D 2V	5 D 1	6 D 2V	6 D 0.	7 D 0	7 D 0	6 D 0	7 D 0	8 D 0	8 D 0	10 D 0	8 D 0	8 D 0	8 D 0
1-11Z	5 D 2V	5 D 1	6 D 0.	6 D 0	8 D 0	8 D 0	8 D 0	9 D 0	8 D 0	8 D 0	10 D 0	8 D 0	7 D 0	6 D 0	4'E 0
1-12Z	6 D 0.	6 D 0	7 D 0	8 D 0	7 D 0	8 D 0	9 D 0	7 D 0	8 D 0	9 D 0	6 D 0	5 D 0	6 D 0	4 E 0	3 D 0

Figure 6. A sample from the computer code output: number of stations, wind availability, and Pasquill stability for each segment. The right hand portion of the table, segments 16 through 24, has been deleted.

START DATE-TIME DEC 75	TRAJECTORY SEGMENT 1 25	2 26	3 27	4 28	5 29	6 30	7 31	8 32	9 33	10 34	11 35	12 36	13 37	14 38	15 39
1- 0Z	1 120	3 120	4 120	5 120	6 120	7 120	8 120	10 120	10 120	13 120	13 120	13 120	15 120	15 9999	15 9999
1- 1Z	3 120	4 120	5 120	6 120	7 120	8 120	10 120	10 120	13 120	13 120	13 120	15 120	15 9999	15 9999	18 9999
1- 2Z	3 120	4 120	5 120	7 120	8 120	10 120	10 120	10 120	13 120	13 120	13 120	15 9999	15 9999	18 9999	18 9999
1- 3Z	4 120	4 120	6 120	7 120	8 120	10 120	10 120	13 120	13 120	13 120	15 9999	15 9999	15 9999	18 9999	118 9999
1- 4Z	3 118	4 120	6 120	7 120	8 120	10 120	10 120	13 120	13 120	13 9999	15 9999	15 9999	15 9999	18 9999	118 9999
1- 5Z	4 118	5 118	7 118	8 120	10 120	10 120	10 120	13 120	13 120	13 120	15 9999	15 9999	15 9999	18 9999	118 9999
1- 6Z	4 118	5 118	7 118	8 120	10 120	10 120	10 120	13 120	13 120	13 9999	15 9999	15 9999	15 9999	15 9999	118 9999
1- 7Z	4 118	5 118	7 118	8 118	10 120	10 120	10 120	13 120	13 120	13 9999	15 9999	15 9999	15 9999	15 9999	118 9999
1- 8Z	4 118	5 118	7 118	8 118	10 120	10 120	10 120	13 9999	13 9999	13 9999	15 9999	15 9999	15 9999	15 9999	118 9999
1- 9Z	4 118	5 118	7 118	8 118	10 120	10 9999	10 9999	13 9999	13 9999	13 9999	15 9999	15 9999	15 9999	15 9999	118 9999
1-10Z	4 118	5 118	7 118	8 118	10 9999	10 9999	10 9999	13 9999	13 9999	13 9999	15 9999	15 9999	15 9999	15 9999	118 9999
1-11Z	4 118	5 118	7 9999	8 9999	10 9999	10 9999	10 9999	13 9999	13 9999	13 9999	15 9999	15 9999	15 9999	15 9999	15 9999
1-12Z	4 9999	5 9999	7 9999	8 9999	10 9999	10 9999	10 9999	13 9999	13 9999	13 9999	15 9999	15 9999	15 9999	15 9999	15 9999

Figure 7. A sample from the computer code output: the height (hundredths of meters) of the bottom and top of the transport layer. The right hand portion of the table, segments 16 through 24, has been deleted.

START DATE-TIME DEC 75	TRAJECTORY SEGMENT 1 25	 2 26	 3 27	 4 28	 5 29	 6 30	 7 31	 8 32	 9 33	 10 34	 11 35	 12 36	 13 37	 14 38	 15 39
1- 0Z	735 453	734 453	1540 453	2040 453	2040 453	2040 453	2040 453	2053 453	2053 753	2053 1153	2053 1153	2053 1153	2053 1154	2053 9999	2053 9999
1- 1Z	734 453	734 453	2040 453	2040 453	2040 453	2040 453	2053 453	2053 753	2053 1153	2053 1153	2053 1153	2053 1154	2053 9999	2053 9999	453 9999
1- 2Z	734 453	2040 453	2040 453	2040 453	2040 453	2053 453	2053 753	2053 1153	2053 1153	2053 1153	2053 1154	2053 9999	2053 9999	453 9999	453 9999
1- 3Z	734 453	2040 453	2040 453	2040 453	2053 453	2053 753	2053 1153	2053 1153	2053 1153	2053 1154	2053 9999	453 9999	453 9999	453 9999	453 9999
1- 4Z	753 453	2040 453	2040 453	2053 453	2053 753	2053 1153	2053 1153	2053 1153	2053 1154	2053 9999	453 9999	453 9999	453 9999	453 9999	453 9999
1- 5Z	753 453	2040 453	2053 453	2053 753	2053 1153	2053 1153	2053 1153	2053 1154	2053 1154	453 1154	453 9999	453 9999	453 9999	453 9999	453 9999
1- 6Z	753 453	2053 453	2053 753	2053 1153	2053 1153	2053 1153	2053 1154	753 1154	453 1154	453 9999	453 9999	453 9999	453 9999	453 9999	453 9999
1- 7Z	753 453	2053 753	2053 1153	2053 1153	2053 1153	2053 1154	753 1154	453 1154	453 754	453 9999	453 9999	453 9999	453 9999	453 9999	453 9999
1- 8Z	753 753	2053 1153	2053 1153	753 1153	755 1154	753 1154	453 1154	453 9999	453 9999	453 9999	453 9999	453 9999	453 9999	453 9999	453 9999
1- 9Z	753 1153	2053 1153	753 1153	755 1154	753 1154	453 9999	453 9999	453 9999	453 9999	453 9999	453 9999	453 9999	453 9999	453 9999	453 9999
1-10Z	753 1153	753 1153	755 1154	753 1154	453 9999	453 9999	453 9999	453 9999	453 9999	453 9999	453 9999	453 9999	453 9999	453 9999	453 9999
1-11Z	753 1153	755 1154	753 9999	453 9999	453 9999	453 9999	453 9999	453 9999	453 9999	453 9999	453 9999	453 9999	453 9999	453 9999	453 9999
1-12Z	755 9999	753 9999	453 9999	453 9999	453 9999	453 9999	453 9999	453 9999	453 9999	453 9999	453 9999	453 9999	453 9999	453 9999	453 9999

Figure 8. A sample from the computer code output: the height (hundredths of meters) of the lowest and highest stable layer. The right hand portion of the table, segments 16 through 24, has been deleted.

START DATE-TIME DEC 75	TRAJECTORY SEGMENT 1 / 25	2 / 26	3 / 27	4 / 28	5 / 29	6 / 30	7 / 31	8 / 32	9 / 33	10 / 34	11 / 35	12 / 36	13 / 37	14 / 38	15 / 39
1- 0Z	214	-3008	-2409	-2109	-2009	-1909	-1810	-1610	-1710	-112	-212	-212	113	-213	-213
	-1123	-1322	-1622	-2122	-2621	-3021	-3420	-3819	0	0	0	0	-4414	9999	9999
1- 1Z	-3008	-2508	-2109	-1909	-1810	-1710	-1610	-1710	-112	-112	-112	113	-213	-214	-314
	-1322	-1722	-2122	-2621	-3021	-3420	-3819	0	0	0	0	0	9999	9999	9999
1- 2Z	-2708	-2209	-2009	-1710	-1710	-1610	-1610	-1610	-112	-112	213	-213	-214	-314	-315
	-1722	-2122	-2621	-3021	-3520	-3819	0	0	0	0	0	-4414	9999	9999	9999
1- 3Z	-2109	-2109	-1710	-1610	-1510	-1510	-1510	-112	-113	213	-213	-214	-214	-315	-416
	-2021	-2521	-2920	-3420	-3819	-4118	0	0	0	-4414	9999	9999	9999	9999	9999
1- 4Z	-2308	-1809	-1510	-1510	-1510	-1411	-1411	-113	213	-113	-214	-214	-214	-416	-616
	-1219	-2920	-3320	-3719	-4018	0	0	0	-4313	9999	9999	9999	9999	9999	9999
1- 5Z	-1709	-1510	-1311	-1411	-1411	-1411	-1211	213	-113	-114	-214	-215	-315	-616	-1017
	-1619	-2018	-2317	-4018	-4417	0	0	-4414	0	0	9999	9999	9999	9999	9999
1- 6Z	-1609	-1410	-1311	-1311	-1311	-1212	-611	-113	-114	-114	-215	-315	-515	-716	-1617
	-2018	-2317	-2616	-4417	0	0	-4414	0	0	9999	9999	9999	9999	9999	9999
1- 7Z	-1410	-1410	-1311	-1311	-1112	-611	-912	-114	-114	-114	-315	-515	-716	-1216	-2317
	-2317	-2616	-2916	0	0	-4514	0	0	0	9999	9999	9999	9999	9999	9999
1- 8Z	-1310	-1210	-1211	-1012	-512	-813	-613	-114	-115	-214	-515	-816	-1216	-1715	-2815
	-2516	0	0	0	-4414	0	0	9999	9999	9999	9999	9999	9999	9999	9999
1- 9Z	-1210	-1211	-912	-412	-713	-613	-513	-115	-215	-315	-916	-1316	-1815	-2014	-3013
	0	0	0	-3213	0	9999	9999	9999	9999	9999	9999	9999	9999	9999	9999
1-10Z	-1210	-911	-412	-613	-514	-514	-414	-215	-415	-615	-1416	-1915	-2014	-1812	20
	0	0	-3213	0	9999	9999	9999	9999	9999	9999	9999	9999	9999	9999	9999
1-11Z	-1110	-611	-412	-312	-514	-414	-314	-416	-716	-1015	-1915	-2014	-1812	1319	1019
	0	-3314	9999	9999	9999	9999	9999	9999	9999	9999	9999	9999	9999	9999	9999
1-12Z	-810	-511	-312	-313	-414	-314	-314	-816	-1115	-1214	-2014	-1812	1319	919	619
	9999	9999	9999	9999	9999	9999	9999	9999	9999	9999	9999	9999	9999	9999	9999

Figure 9. A sample from the computer code output: wind direction change and wind speed shear. The right hand portion of the table, segments 16 through 24, has been deleted.

START DATE-TIME DEC 75	DURATION (HOURS) 3 / 33		6 / 36		9 / 39		12 / 42		15 / 45		18 / 48	
1- 0Z	3335	8180	3361	8206	3396	8210	3418	8168	3422	8121	3408	8067
	3158	7907	3130	7861	9999	9999	9999	9999	9999	9999	9999	9999
1- 1Z	3340	8190	3369	8208	3404	8206	3415	8152	3414	8103	3393	8047
	3149	7889	3120	7848	9999	9999	9999	9999	9999	9999	9999	9999
1- 2Z	3344	8191	3380	8206	3411	8185	3421	8131	3414	8082	3373	8040
	3139	7875	9999	9999	9999	9999	9999	9999	9999	9999	9999	9999
1- 3Z	3353	8190	3391	8196	3415	8158	3425	8108	3415	8059	3361	8025
	3123	7871	9999	9999	9999	9999	9999	9999	9999	9999	9999	9999
1- 4Z	3356	8181	3394	8189	3413	8139	3417	8088	3399	8039	3344	8003
	3130	7847	9999	9999	9999	9999	9999	9999	9999	9999	9999	9999
1- 5Z	3364	8182	3401	8168	3422	8113	3418	8066	3380	8032	3338	7985
	3113	7852	9999	9999	9999	9999	9999	9999	9999	9999	9999	9999
1- 6Z	3366	8178	3401	8150	3422	8096	3415	8055	3363	8024	3334	7975
	3102	7846	9999	9999	9999	9999	9999	9999	9999	9999	9999	9999
1- 7Z	3365	8181	3398	8129	3416	8073	3401	8032	3350	8001	3311	7967
	3088	7841	9999	9999	9999	9999	9999	9999	9999	9999	9999	9999
1- 8Z	3364	8152	3408	8087	3412	8040	3379	8012	3339	7970	3287	7954
	9999	9999	9999	9999	9999	9999	9999	9999	9999	9999	9999	9999
1- 9Z	3364	8134	3396	8074	3397	8040	3352	8002	3322	7954	3253	7956
	9999	9999	9999	9999	9999	9999	9999	9999	9999	9999	9999	9999
1-10Z	3360	8116	3379	8069	3368	8030	3325	7983	3282	7945	3219	7955
	9999	9999	9999	9999	9999	9999	9999	9999	9999	9999	9999	9999
1-11Z	3353	8115	3361	8071	3335	8023	3301	7958	3241	7945	3189	7949
	9999	9999	9999	9999	9999	9999	9999	9999	9999	9999	9999	9999
1-12Z	3336	8117	3339	8065	3315	8006	3282	7943	3209	7948	3159	7934
	9999	9999	9999	9999	9999	9999	9999	9999	9999	9999	9999	9999

Figure 10. A sample from the computer code output: positions of trajectory segment endpoints. The right hand portion of the table, hours 18 through 30, has been deleted.

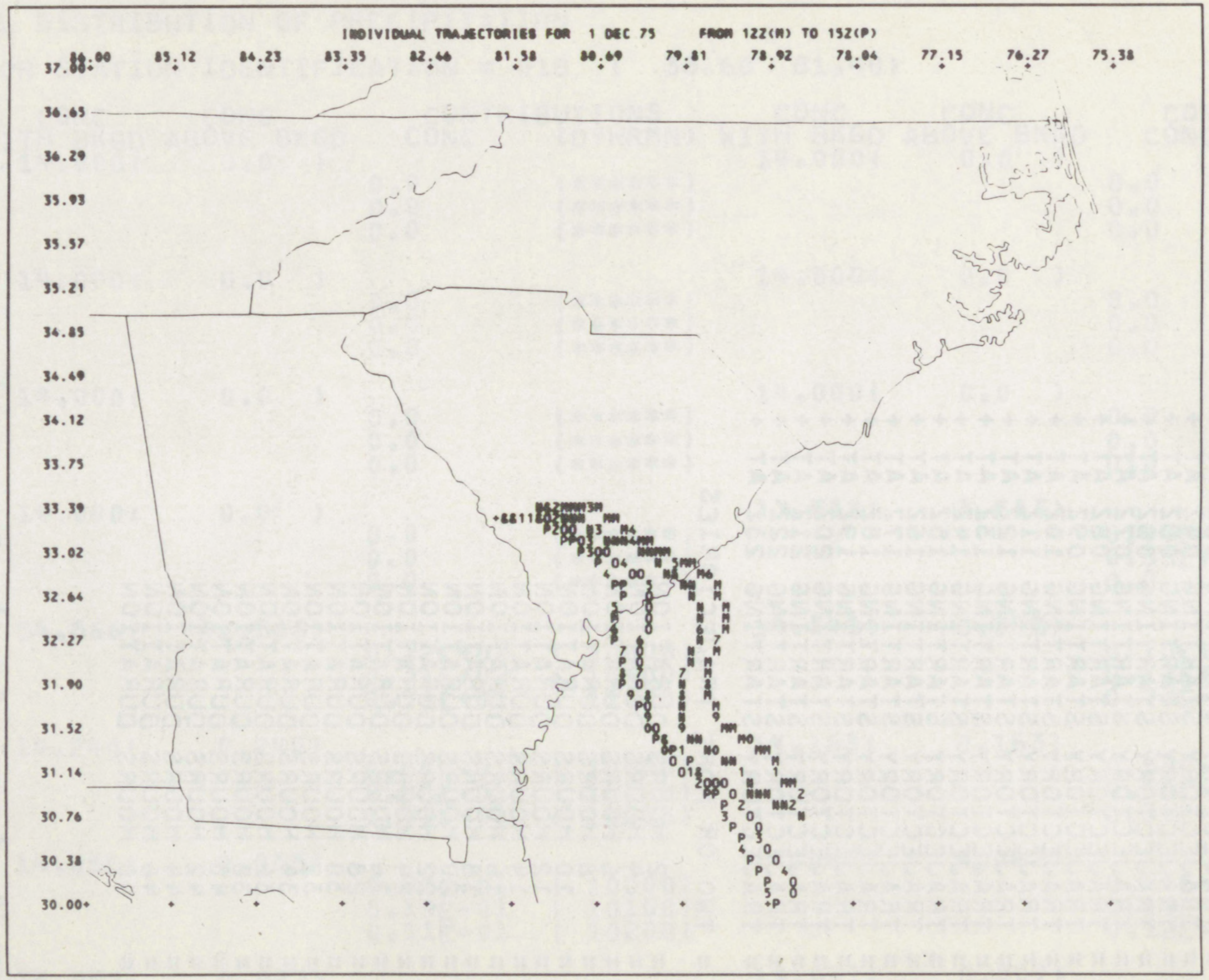

Figure 11. A sample from the computer code output: trajectory mercator plot for trajectories starting at 12Z (M), 13Z (N), 14Z (O), and 15Z (P).

```
TRAJECTORY SEGMENT MERCATOR MAP SYMBOL TABLE

A = TRAJECTORY STARTING 00Z AT +
B = TRAJECTORY STARTING 01Z AT +
C = TRAJECTORY STARTING 02Z AT +
D = TRAJECTORY STARTING 03Z AT +
E = TRAJECTORY STARTING 04Z AT +
F = TRAJECTORY STARTING 05Z AT +
G = TRAJECTORY STARTING 06Z AT +
H = TRAJECTORY STARTING 07Z AT +
I = TRAJECTORY STARTING 08Z AT +
J = TRAJECTORY STARTING 09Z AT +
K = TRAJECTORY STARTING 10Z AT +
L = TRAJECTORY STARTING 11Z AT +
M = TRAJECTORY STARTING 12Z AT +
N = TRAJECTORY STARTING 13Z AT +
O = TRAJECTORY STARTING 14Z AT +
P = TRAJECTORY STARTING 15Z AT +
Q = TRAJECTORY STARTING 16Z AT +
R = TRAJECTORY STARTING 17Z AT +
S = TRAJECTORY STARTING 18Z AT +
T = TRAJECTORY STARTING 19Z AT +
U = TRAJECTORY STARTING 20Z AT +
V = TRAJECTORY STARTING 21Z AT +
W = TRAJECTORY STARTING 22Z AT +
X = TRAJECTORY STARTING 23Z AT +

& = TWO OR MORE TRAJECTORIES

1 =  2 HOURS DURATION
2 =  4 HOURS DURATION
3 =  6 HOURS DURATION
4 =  8 HOURS DURATION
5 = 10 HOURS DURATION
6 = 12 HOURS DURATION
7 = 14 HOURS DURATION
8 = 16 HOURS DURATION
9 = 18 HOURS DURATION
0 = 20 HOURS DURATION
1 = 22 HOURS DURATION
2 = 24 HOURS DURATION
3 = 26 HOURS DURATION
4 = 28 HOURS DURATION
5 = 30 HOURS DURATION
6 = 32 HOURS DURATION
7 = 34 HOURS DURATION
8 = 36 HOURS DURATION
9 = 38 HOURS DURATION
0 = 40 HOURS DURATION
1 = 42 HOURS DURATION
2 = 44 HOURS DURATION
3 = 46 HOURS DURATION
4 = 48 HOURS DURATION
```

Figure 12. A sample from the computer code output: trajectory mercator plot symbol table.

```
BOX MODEL DIFFUSION            VD=  0.0 CM/S            PRECIPITATION= 105.7 CM/YR

SPATIAL DISTRIBUTION OF PRECIPITATION

RECEPTOR STATION IDENTIFICATION = 010  (  33.60  81.40)

        CONC      CONC          CONTRIBUTIONS         CONC      CONC          CONTRIBUTIONS
DATE WITH BKGD ABOVE BKGD     CONC        (DYHRMN) WITH BKGD ABOVE BKGD     CONC        (DYHRMN)
100   14.000(    0.0   )                            14.000(    0.0   )
                             0.0         (******)                          0.0         (******)
                             0.0         (******)                          0.0         (******)
                             0.0         (******)                          0.0         (******)

103   14.000(    0.0   )                            14.000(    0.0   )
                             0.0         (******)                          0.0         (******)
                             0.0         (******)                          0.0         (******)
                             0.0         (******)                          0.0         (******)

106   14.000(    0.0   )                            14.000(    0.0   )
                             0.0         (******)                          0.0         (******)
                             0.0         (******)                          0.0         (******)
                             0.0         (******)                          0.0         (******)

109   14.000(    0.0   )                            17.513(    3.513)
                             0.0         (******)                          0.47E-02    ( 10000)
                             0.0         (******)                          0.35E+01    ( 10800)
                             0.0         (******)                          0.0         (******)

112   56.566(   42.566)                             14.342(    0.342)
                             0.12E+01    ( 10800)                          0.10E+00    ( 10000)
                             0.31E+02    ( 10900)                          0.12E+00    ( 10100)
                             0.96E+01    ( 11000)                          0.73E-01    ( 10200)

115   14.240(    0.240)                             14.163(    0.163)
                             0.84E-01    ( 10000)                          0.58E-01    ( 10000)
                             0.85E-01    ( 10100)                          0.58E-01    ( 10100)
                             0.51E-01    ( 10200)                          0.34E-01    ( 10200)

118   14.055(    0.055)                             14.062(    0.062)
                             0.20E-01    ( 10000)                          0.21E-01    ( 10000)
                             0.19E-01    ( 10100)                          0.19E-01    ( 10100)
                             0.11E-01    ( 10200)                          0.12E-01    ( 10200)

121   14.027(    0.027)                             14.007(    0.007)
                             0.87E-02    ( 10000)                          0.26E-02    ( 10000)
                             0.77E-02    ( 10100)                          0.21E-02    ( 10100)
                             0.47E-02    ( 10200)                          0.12E-02    ( 10200)
```

Figure 13. A sample from the computer code output: receptor diffusion model. The right hand portion of the table has been deleted. Sampling times of 02, 05, 08, 11, 14, 17, and 23 h GMT are not shown.